POWER DIAGRAMS AND THEIR APPLICATIONS

D. SIERSMA AND M. VAN MANEN

ABSTRACT. We remark that the power diagrams from computer science are the spines of amoebas in algebraic geometry, or the hypersurfaces in tropical geometry. Our concept of a Morse poset generalizes to power diagrams. We show that there exists a discrete Morse function on the coherent triangulation, dual to the power diagram, such that its critical set equals the Morse poset of the power diagram. In the final section we use Maslov dequantization to compute the medial axis.

1. INTRODUCTION

Power diagrams were introduced by Aurenhammer in [Aur87], as a generalization of the more commonly known Voronoi diagrams. They recently surfaced in algebraic geometry, as the spines of amoebas, see [PR04]. Another appearance of the power diagram is what other authors call a tropical hypersurface, see [RGST03]. They also appear when string theorists use toric geometry, see for instance [DFG02].

The treatment they receive in [PR04] is different from the one in [Aur87]. The essential tool that Passare and Rullgård use is the Legendre transform, a tool that first seems to have been introduced in convex analysis in [Man39]. The essential tool that Aurenhammer uses is that the power diagram of some points in $\mathbb{R}^n$ is a projection of a convex hull in $\mathbb{R}^{n+1}$. We spell out the relation between the classical theory of Voronoi diagrams and that of the tropical hypersurface. Note that what we call here a Delaunay triangulation is called a coherent triangulation in chapter 7 of [GKZ94]. Such triangulations are called regular in [Zie95].

After that we will explore the relationship between Voronoi diagrams and power diagrams. In particular given a power diagram $\mathcal{T}$ of N points $\{P_1, \cdots, P_N\}$ in $\mathbb{R}^n$ we will construct a Voronoi diagram Υ of N points in $\mathbb{R}^{n+1}$ a hyperplane section of which is the diagram $\mathcal{T}$. Thus power diagrams are affine Voronoi diagrams in a very precise sense.

Then we focus on higher order structures. With a Voronoi diagram there come the k-th order Voronoi diagrams and the Delaunay triangulation. The k-th order power diagram is again a power diagram, see [AI87], and to it there is associated the k-th order coherent triangulation. The union of all the power diagrams is a hyperplane arrangement. We conclude that not every picture that looks like a power diagram is actually a power diagram.

The main new point of view we present in this article is the relation between tropical hypersurfaces and discrete Morse theory introduced by Forman in [For98]. This seems to have gone unnoticed before. The triangulations are polyhedral complexes, and the affine linear functions that define the power diagram give rise to discrete Morse function on the dual simplicial complex. We apply this third way of looking at power diagrams to a notion we introduced before, the Morse poset. Morse posets are seen to be determining a discrete vectorfield.

We apply our newly found knowledge to the problem of enumerating different Morse posets.

In the final section we show another application of tropical geometry to computational geometry. We use Maslov dequantization to determine the medial axis.

Many of our results can in some explicit form or another be found in the literature. We have gone to great lengths to include appropriate references, but in all likelihood we are not complete. It has been remarked by other authors also that many results in tropical geometry - as the field has come to be known - are just well-known theorems from other fields, but now in a different guise. This article just reinforces that opinion.

2. Power diagrams and tropical hypersurfaces.

In this section we show the equivalence of two definitions of the power diagram. First we discuss the original notion of Aurenhammer, then we show that these are equivalent to the definitions of Passare *et. al.*.

2.1. **The definition of Aurenhammer.** The original definition of a power diagram is by means of distance function with weights. Take a point set $\{P_1, \cdots, P_N\} \subset \mathbb{R}^n$. Throughout this article we assume that $\dim(\mathrm{CH}(\{P_1, \cdots, P_N\})) = n$. Assign a weight w_i to each point P_i. Then write down the functions:

$$(1) \qquad g_i \colon \mathbb{R}^n \to \mathbb{R} \quad g_i(x) = \frac{1}{2}\|x - P_i\| - \frac{1}{2}w_i \quad g(x) = \min_{1 \le i \le N} g_i(x)$$

Here we have used the following notation:

$$\|x\| = \sum_{i=1}^n x_i^2$$

DEFINITION 1. *For a subset $\alpha \subset \{P_1, \cdots, P_N\}$ the set $\mathrm{Pow}(\alpha)$ is the closure of*

$$\{x \in \mathbb{R}^n \mid g_i(x) = g(x) \ P_i \in \alpha \ and \ g_j(x) > g(x) \ P_j \notin \alpha\}$$

The sets $\mathrm{Pow}(\{P_i\})$ are sometimes called cells.

The separator $\mathrm{Sep}(\{P_i, P_j\})$ between P_i and P_j is the hyperplane.

$$\{x \in \mathbb{R}^n \mid g_i(x) = g_j(x)\}$$

It is no restriction to assume that $w_i > 0$. We may add some number to all of the functions g_i: the cells will not change. In fact we can add any function $h \colon \mathbb{R}^n \to \mathbb{R}$ to the g_i. We will get the same power diagram. Power diagrams are polyhedral subdivisions. We repeat definition 1 in [PR04].

DEFINITION 2. *A polyhedral subdivision $\mathcal{T}$ of a polyhedron $K \subset \mathbb{R}^n$ is a subdivision of K in polyhedra K_i, such that*

- *The union of all sets $K_i \in \mathcal{T}$ is K.*
- *If K_i and K_j are both in $\mathcal{T}$ then so is their intersection.*
- *Every compact subset L of K intersects only a finite number of the K_i.*

THEOREM 1. *The sets $\mathrm{Pow}(\alpha)$ for $\alpha \subset \{P_1, \cdots, P_N\}$ are a polyhedral subdivision of $\mathbb{R}^n$. This polyhedral subdivision is called the* power diagram.

Proof. The cells cover $\mathbb{R}^n$. They are the intersection of a finite number of halfspaces of the form: $\{x \in \mathbb{R}^n \mid g_i(x) \leq g_j(x)\}$. So they are polyhedra. $\qquad\square$

Besides many similarities , there are a few crucial differences between power diagrams and Voronoi diagrams. In a power diagram the cell of a point may well be empty. It might happen that $g_i(x) > g_j(x)$, for all $i \neq j$ and all $x \in \mathbb{R}^n$.

Also, whereas in Voronoi diagrams, P_i is always contained in its own cell, in a power diagram the cell of P_i might not be empty and still P_i does not lie in its own cell!

The power diagram can be constructed much like the Voronoi diagram. Recall that the Voronoi diagram is the upper convex hull to the tangent planes to a parabola $x_0 = a(\sum_{i=1}^{n} x_i^2)$. For the case of the power diagrams we do much the same thing. Look at figure 1. We take cylinders with radius $\sqrt{w_i}$ around the lines $x = P_i$ in $\mathbb{R}^{n+1}$. The intersection of the cylinders with the parabola is a torsion zero space curve. We draw the planes in which they lie (left figure) and we consider the upper convex hull of these planes (right figure). The projection of its singular sides is the power diagram.
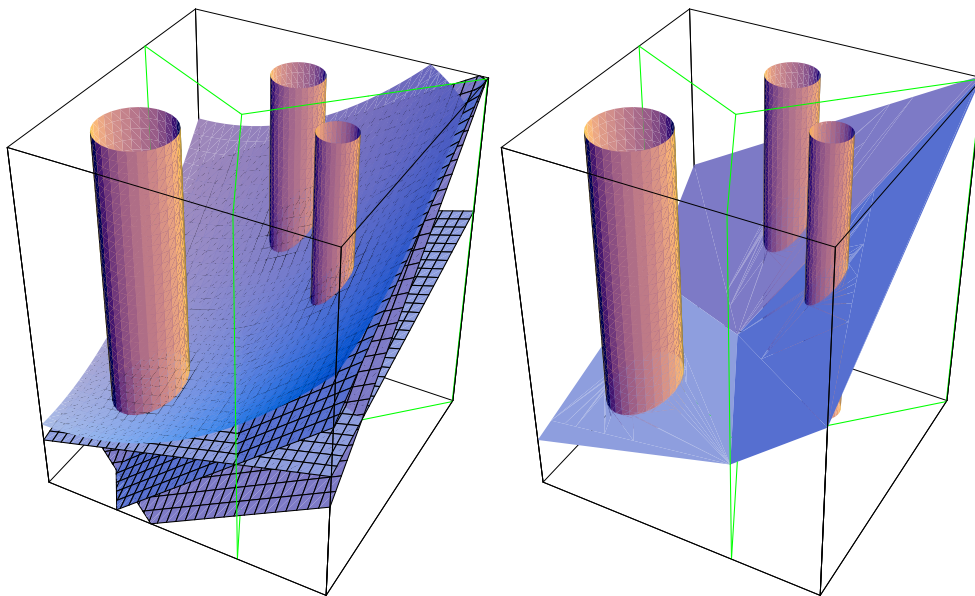

FIGURE 1. Power lifting to the parabola

The above construction is also described in [Aur87], section 4.1. When the $r_i = 0$ the construction reduces to the well-known construction of Voronoi diagrams. In that case, of course, one has to take the tangent planes to the paraboloid.

2.2. **Tropical hypersurface.** The power diagram can be defined using only affine functions. With amoebas in mind, this was done in [PR04]. With tropical hypersurfaces in mind, this was done in [RGST03]. The separator between P_i and P_j is a hyperplane. It is given by

$$g_i(x) = g_j(x) \Leftrightarrow \langle x, P_i \rangle - \frac{\|P_i\| - w_i}{2} = \langle x, P_j \rangle - \frac{\|P_j\| - w_j}{2}$$

We can define the power diagram solely using the affine functions $f_i(x) = \langle x, P_i \rangle + c_i$, where the coefficient c_i is

$$(2) \qquad\qquad c_i = -\frac{\|P_i\| - w_i}{2}$$

Consider the function

$$f(x) = \max_{i=1,\cdots,N} f_i(x)$$

The following proposition shows that we can define the power diagram solely using affine functions.

PROPOSITION **1.** *For a subset $\alpha \subset \{P_1, \cdots, P_N\}$ the set $\mathrm{Pow}(\alpha)$ is the closure of*

$$\{x \in \mathbb{R}^n \mid f_i(x) = f(x) \ P_i \in \alpha \text{ and } f_j(x) < f(x) \ P_j \notin \alpha\}$$

REMARK **1.** *In* [RGST03], *f is defined as the minimum of the functions f_i. Taking the minimum or taking the maximum is just a convention though.*

The affine definition of power diagrams is more elegant. We lose the immediate appeal of the construction in figure 1, but two statements are now immediately clear.

PROPOSITION **2.** *The intersection of a hyperplane with a power diagram is again a power diagram. The image of a power diagram under an affine map $\mathbb{R}^n \to \mathbb{R}^n$ is again a power diagram.*

So a power diagram can be sliced, after which we obtain a new power diagram. In fact, every power diagram in $\mathbb{R}^n$ is a slice of a Voronoi diagram in $\mathbb{R}^{n+1}$.

PROPOSITION **3.** *Let $\mathcal{T}$ be a power diagram in $\mathbb{R}^n$. There is a Voronoi diagram Υ in $\mathbb{R}^{n+1}$ and a hyperplane H such that $H \cap \Upsilon = \mathcal{T}$.*

Proof. We will explicitly construct such an Υ. Let $\{P_1, \cdots, P_N\}$ be the set of points in $\mathbb{R}^n$ that determine $\mathcal{T}$. Write

$$Q_i = (P_i, P_i') \quad \bar{x} = (x, x')$$

We have

$$\|\bar{x} - Q_i\| = \|x - P_i\| + (x' - P_i')^2$$

So when $x' = 0$ we get

$$\|\bar{x} - Q_i\| = \|x - P_i\| + P_i'^2$$

Now let the power diagram be given by functions g_i as in equation (1). It is no restriction to assume that $w_i < 0$, because only the differences $w_i - w_j$ matter for the power diagram. Thus we can choose $P_i' = \sqrt{-w_i} = r_i$. □

2.3. The Legendre transform.

Dual to the Voronoi diagram is the Delaunay triangulation. In a similar way there exists a dual of the power diagram. This dual cell complex is not always a triangulation, similar to the case with the Delaunay triangulation. If we use the tropical point of view (with affine functions) we can best explain the dual object using the Legendre transform, see [Hör94], which we explain below. This dual object is also considered in [GKZ94], where it has the name coherent triangulation.

We start with some definitions. Let P be a polyhedron in $\mathbb{R}^{n+1}$. Let v be a vector in $\mathbb{R}^n$. The *lower faces* of P with respect to v are those faces F of P such that

$$\forall x \in F \ \forall \lambda \in \mathbb{R}_{>0} \colon x - \lambda v \notin P$$

A polyhedral subdivision of a polytope in $\mathbb{R}^n$ is called *regular* if it is the projection of the lower faces of a polytope in $\mathbb{R}^{n+1}$. Not every polyhedral subdivision is regular, see chapter 5 in [Zie95], or chapter 7 in [GKZ94].

DEFINITION 3. *The Legendre transform of a convex function f, with domain $D \subset \mathbb{R}^n$ is*

$$\hat{f}(\xi) = \sup_{x \in D} \left(\langle \xi, x \rangle - f(x) \right)$$

When the supremum does not exists, we put $\hat{f}(\xi) = \infty$. The domain $\mathrm{Dom}(\hat{f})$ of $\hat{f}$ are those ξ for which $\hat{f}(\xi) < \infty$.

The Legendre transform of $f(x) = \frac{1}{2}\|x\|$ is the function itself. The Legendre transform of a linear function $f_i = \langle x, P_i \rangle + c_i$ is $< \infty$ only when $\xi = P_i$. Theorem 2.2.7 of [Hör94] reads:

THEOREM 2. *Let $f = \sup_{\alpha \in A} f_\alpha(x)$ be the maximum of a number of lower semi-continuous convex function. Then f is also a lower semi-continuous convex function. Furthermore $\hat{f}$ is the infimum over all finite sums:*

$$\hat{f}(\xi) = \inf_{\sum \lambda_\alpha \xi_\alpha = \xi, \lambda_\alpha > 0, \sum_\alpha \lambda_\alpha = 1} \sum_\alpha \lambda_\alpha \hat{f}_\alpha(\xi_\alpha)$$

With theorem 2 we calculate the Legendre transform of the function that determines the power diagram. We have

$$f = \max_{1 \leq i \leq N} \langle x, P_i \rangle + c_i$$

The domain where $\hat{f} < \infty$ is the convex hull of the points $\{P_1, \cdots, P_N\}$. We have

$$\hat{f}_i(P_i) = -c_i \Rightarrow \hat{f}(\xi) = \inf \left(-\sum_i \lambda_i c_i \right)$$

where the infimum is taken over all λ_i such that

$$\sum_{1 \leq i \leq N} \lambda_i P_i = \xi \text{ and } \forall i \colon \lambda_i \geq 0 \text{ and } \sum_{i=1}^{N} \lambda_i = 1$$

It is no restriction to assume that only $\leq n+1$ of the λ_i are non-zero because any point in the convex hull of the P_i can be expressed as a sum of $\dim \mathrm{CH}(\{P_1, \cdots, P_N\})$ of the P_i. The infima are best thought of in a geometric way. Take the convex hull $\mathrm{CH}(\{(P_i, -c_i)\}_{i=1}^N)$. The lower faces form the graph of $\hat{f}$ over the convex hull $\mathrm{CH}(\{P_1, \cdots, P_N\})$. We summarize our discussion in a theorem.

THEOREM **3.** *Let* $\mathcal{T}$ *be a power diagram. Let* Υ *be the lower convex hull of the lifted points* $(P_i, -c_i)$ *wrt. to the vector* $(0, \cdots, 0, 1)$. *The polyhedral complex* Υ *is the graph of the Legendre transform* $\hat{f}$ *of* f. *The domain* $\mathrm{Dom}(\hat{f})$ *of* $\hat{f}$ *is the convex hull* $\mathrm{CH}(\{P_1, \cdots, P_N\})$.

The geometrical construction is directly related to the construction of figure 1. If we put the upper convex hull of theorem 3 in figure 1 we get figure 2. What exactly happens
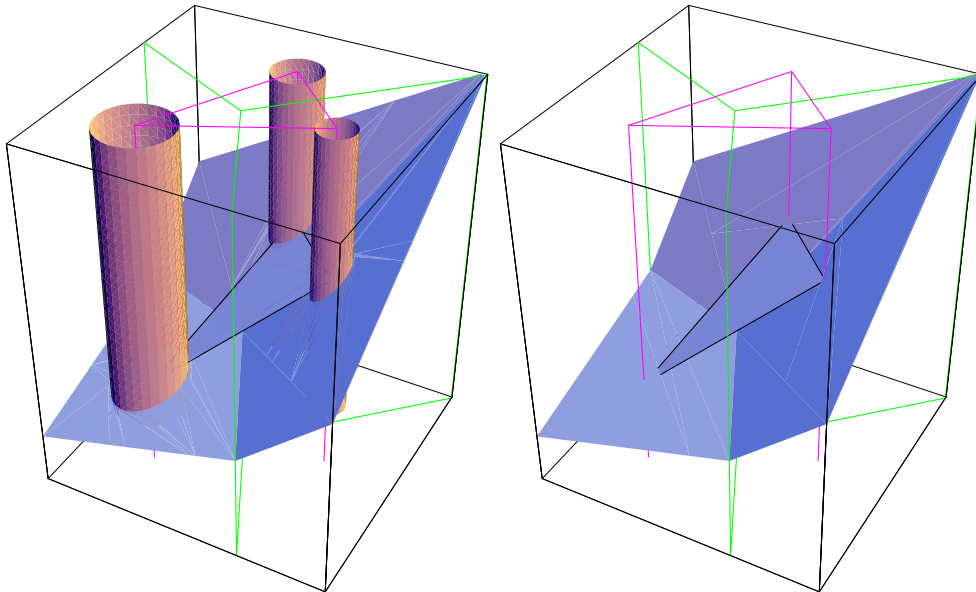

FIGURE 2. The power lift and the Legendre transform

here can best understood by writing out the equations. In figure 1 the graph of $x_0 = \frac{1}{2}\|x\|$ is drawn. Then the cylinders in the picture are $\|x - P_i\| = r_i^2$. Or $\|x - P_i\| = w_i$. Hence the three planes of which we determine the upper hull are

$$(3) \qquad\qquad x_0 = \langle x, P_j \rangle + \frac{r_j^2 - \|P_j\|}{2}$$

The triangle in figure 2 is the plane $x_0 = -\sum \lambda_i c_i$ where the λ_i are defined by $x = \sum \lambda_i P_i$. In the point P_i we have that the graph of $f(x) = \max_i f(x)$ lies $\frac{w_i}{2}$ above the paraboloid $x_0 = \frac{1}{2}\|x\|$, whilst the graph of $\hat{f}(\xi)$ lies $\frac{w_i}{2}$ below the paraboloid there.

Theorem 3 gives a dual triangulation of the power diagram.

DEFINITION 4. *Given a power diagram $\mathcal{T}$ specified by N affine functions, the coherent triangulation σ is the set of points $\xi \in \mathrm{CH}(\{P_1, \cdots, P_N\})$ where $\hat{f}$ is not differentiable.*

Since the coherent triangulation is the projection of the lower convex hull, it has also the structure of a polyhedral complex. In the case when all the weights w_i are zero this coherent triangulation is of course the Delaunay triangulation.

A number of points in $\{P_1, \cdots, P_N\}$ in $\mathbb{R}^n$ is affinely in general position when the convex hull of each subset of length $n+1$ of $\{P_1, \cdots, P_N\}$ is full dimensional. For Voronoi diagrams this definition is not sufficient. It might still be that $n + 2$ lie on a sphere. In that case the Delaunay triangulation is not a simplicial complex. For the Delaunay triangulation to really be a triangulation we need that the points $\{Q_1, \cdots, Q_N\}$ are affinely general position in $\mathbb{R}^{n+1}$ where

$$Q_i = (P_i, \frac{1}{2}\|P_i\|)$$

DEFINITION 5. *A power diagram $f = \max f_i$ is* in general position *when the points Q_i are affinely in general position in $\mathbb{R}^{n+1}$. Here*

$$Q_i = (P_i, -c_i), \ 1 \le i \le N$$

The following theorem is left to the reader.

THEOREM 4. *The coherent triangulation is a simplicial complex when the power diagram is in general position.*

Consider the function

$$(\xi, x) \mapsto F(x, \xi) = f(x) + \hat{f}(\xi) - \langle x, \xi \rangle$$

This function hides the *Gateau differential*. Namely, let $h: \mathbb{R}^n \to \mathbb{R}$ be a function. If the limit

$$h'(x; \xi) = \lim_{t \downarrow 0} \frac{h(x + t\xi) - h(x)}{t}$$

exists, it is called the Gateau differential. See [Hör94], theorem 2.1.22. For a convex set $K \subset \mathbb{R}^n$ the *supporting function* of K is the function

$$\xi \mapsto \sup_{x \in K} \langle x, \xi \rangle$$

Theorem 2.2.11. in [Hör94] says that the Gateau differential $\xi \to f'(x; \xi)$ is the supporting function of

$$\{\xi \mid F(x, \xi) = 0\}$$

Let us see an example of what that means. Take ξ to be one of the points of $\{P_1, \cdots, P_N\}$. Then $\hat{f}(P_i) = -c_i$. So the set of x where $F(x, \xi) = 0$ are those for which $f(x) = \langle x, P_i \rangle + c_i$.

The Gateau differential is called Clarke's generalized derivative in [APS97]. The set of which it is the support function is called $\partial f(x)$. It is stated in that article that $\partial f(x)$ is the convex hull of the gradients of the functions f_i for which $f_i(x) = f(x)$.

That last statement and the theorem 2.1.22 are all equivalent to what is neatly formulated in proposition 1 of [PR04]:

THEOREM **5.** *There is a subdivision of the convex hull* $\mathrm{CH}(\{P_1, \cdots, P_N\})$, *dual to the power diagram* $\mathcal{T}$. *The cell* $\mathrm{Del}(\alpha)$ *dual to* $\mathrm{Pow}(\alpha) \in \mathcal{T}$ *is*

$$\mathrm{Del}(\alpha) = \{\xi \mid F(x, \xi) = 0 \quad \forall x \in \mathrm{Pow}(\alpha)\}$$

Reversely

$$\mathrm{Pow}(\alpha) = \{x \mid F(x, \xi) = 0 \quad \forall \xi \in \mathrm{Del}(\alpha)\}$$

REMARK **2.** *Similar statements are in the review by Pennaneac'h, see* [Pen03]. *However Pennaneac'h does not discuss the relation between the figures 1 and 2. Also she does not make clear what the relationship between this theorem and the well-known theory of Voronoi diagrams/ Delaunay tesselations is. Her review however is heartily recommended.*

3. DISAPPEARING FACES

We have noted before that faces in the power diagram might disappear. This will happen for some $P_j \in \{P_1, \cdots, P_N\}$ iff.

$$f_j(x) < f(x) \quad \forall x \in \mathbb{R}^n$$

Cells in the power diagram correspond to vertices in the coherent triangulation. In that case it is very easy to see which vertices disappear. They are the ones lying in the epigraph of the Legendre transform. Remember that the epigraph of a function $h \colon D \to \mathbb{R}$ is defined as:

$$\{(x, t) \mid h(x) < t \quad x \in D\}$$

Let us sum up some consequences:

If P_j lies outside the convex hull of $\mathrm{CH}(\{P_1, \cdots, P_N\} \setminus \{P_j\})$ then the cell $\mathrm{Pow}(\{P_j\})$ is not empty. Proof: the lifted point $(P_j, -c_j)$ forcibly is part of the lower hull of the points $(P_i, -c_i)$.

The transition on the power diagrams where a cell disappears is exemplified in figure 3. In the pictures the convex hull of the points $(P_i, -c_i)$ is drawn. The graph of the Legendre transform $\hat{f}$ is formed by the lower faces of that polytope. In the ground plane we see the projection of those lower faces: the coherent triangulation dual to the power diagram. In the ground plane also the circles with radius $\sqrt{w_i}$ are drawn.

On the left hand side of figure 3 we see a point with a small circle around it. This point disappears when we make one of the circles in the pictures (the one on the upper right) bigger. Such has been done on the left hand side of figure 11. The upper right circle is much bigger there and the lifted point corresponding to the small circle lies inside the epigraph of the Legendre transform $\hat{f}$. We thus see that there are three sorts of events on planar coherent triangulations:

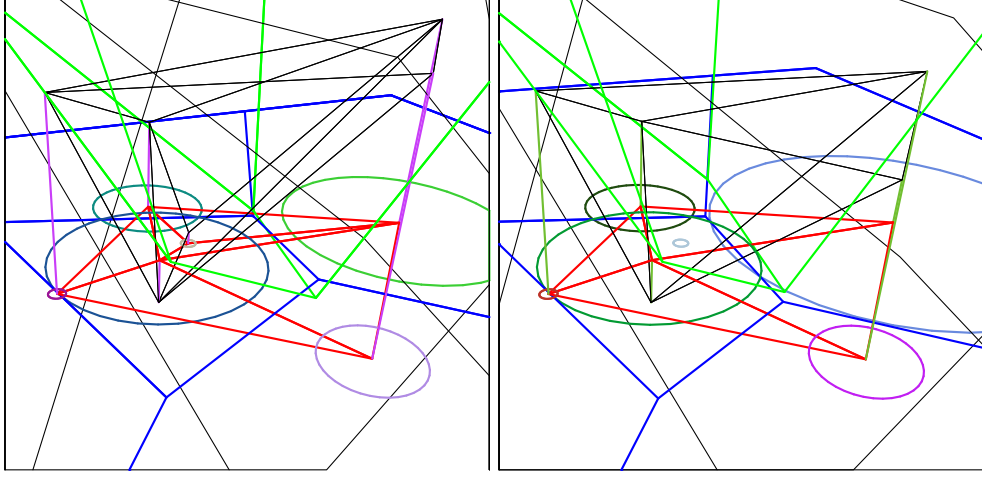- Convex hull events and edge flips
- Disappearing vertices.

FIGURE 3. Transition on power diagrams

Convex hull events and edge flips already occur in families of Voronoi diagrams. A detailed study of these phenomena can be found in [Lin02]. However in a dual triangulation of a Voronoi diagram, none of the cells $\mathrm{Pow}(\{P_i\})$ can be empty.

4. THE k-TH ORDER POWER DIAGRAM AND HYPERPLANE ARRANGEMENTS

Given a power diagram we define a kth order power diagram. Consider all subsets I of length k in $\{1, \cdots, N\}$. Denote

$$P_I = \frac{1}{|I|} \sum_{i \in I} P_i$$

and

$$f_I = \frac{1}{|I|} \sum_{i \in I} f_i = \langle x, P_I \rangle + \frac{1}{|I|} \sum_{i \in I} c_i$$

Denote also

$$f^{(k)} = \max_{I \subset \{1, \cdots, N\}\, |I| = k} f_I$$

So $f^{(1)} = f$.

DEFINITION **6.** *The k-th order power diagram* $\mathrm{Pow}^{(k)}$ *is the power diagram of the f_I. Denote* $\mathrm{Del}^{(k)}$ *its dual.*

Our definition is admittedly rather arbitrary. One can take any weighted sum of the points.

LEMMA **1.** *The k-th order power diagram is a polyhedral complex. The point x lies in the cell I of the k-th power diagram iff. $f_i(x) \geq f_j(x)\ \forall i \in I\ $ and $\forall j \in \{1, \cdots, N\} \setminus I$.*

Proof. The first part of the lemma is obvious. The second part of the lemma boils down to the following obvious statement. Let $\{a_i\}_{i=1}^N$ be a set of real numbers. If I is the index set of the k biggest of the $\{a_i\}_{i=1}^N$ then a_I is the biggest of the numbers

$$\{\frac{1}{k}\sum_{j\in J} a_j \mid |J| = k\}$$

$\square$

There are two sources of cells in $\mathrm{Pow}^{(k+1)}$.

- Let $\mathrm{Pow}^{(k)}(I_1)$ and $\mathrm{Pow}^{(k)}(I_2)$ be two power cells in the k-th order power diagram. Assume that the two cells are adjacent, that is there is an edge between the two vertices in the dual coherent triangulation $\mathrm{Del}^{(k)}$. This means that $I_1 \cap I_2$ has $k+1$ distinct elements. Thus the cell of $I_1 \cap I_2$ in $\mathrm{Pow}^{(k+1)}$ is not empty.
- Let the cell of $I \subset \{P_1, \cdots, P_N\}$ be an empty cell. That is:

$$f_I(x) \le f_J(x) \quad \forall x \in \mathbb{R}^n \quad \forall J \subset \{P_1, \cdots, P_N\} \quad |J| = k$$

but that at some point $x_0 \in \mathbb{R}^n$ there is only one $j \in \{P_1, \cdots, P_N\} \setminus I$ for which $f_j(x_0)$ is bigger than all $f_i(x_0)$ for $i \in I$.
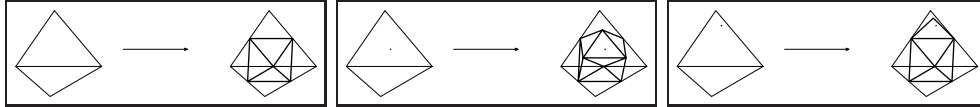

FIGURE 4. A sample of three different kinds of $\mathrm{Del} \to \mathrm{Del}^{(2)}$. If there is a disappeared vertex in Del that vertex may show up in $\mathrm{Del}^{(2)}$. The dots indicate such vertices.

THEOREM **6.** *The union of the power diagrams of order k is a hyperplane arrangement. The hyperplanes are the separators. Each such separator is equipped with a polyhedral subdivision, that is: the separator between P_i and P_j is a hyperplane V divided in at most N closed convex subsets K_l. If x lies in the interior of K_l then x lies on the l-th order power diagram.*

Proof. That there is a polyhedral subdivision on the separator is rather obvious. The points of the k-th diagram is the intersection of two closed convex subsets, so its intersection is also convex. $\square$

The aforementioned hyperplane arrangement is not a generic arrangement. Generically, at most n hyperplanes intersect. In this case, $n + 1$ hyperplanes intersect when they correspond to some cell in a higher order diagram. A hyperplane arrangement does not determine in general a power diagram.

Drawings that look like a power diagram need not be one, just as not all triangulations are coherent. For examples of the latter phenomenon see for instance section 5.1 in [Zie95], where coherent triangulations are called *regular*. As an example of the former, see figure 4. Not all directions will lead to an intersection of the three arrows inside the cell.
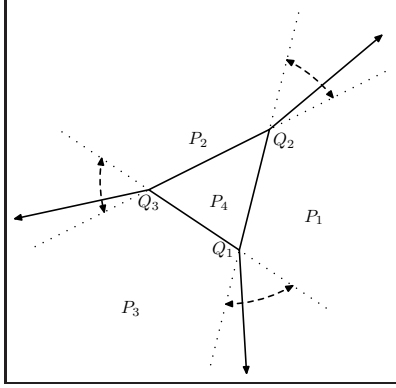
Figure 4:Four regions, marked by P_1, P_2 , P_3 and P_4. $Q_1 = (1, -2)$, $Q_2 = (2, 2)$ and $Q_3 = (-2, 0)$. If the halflines from the Q_i are allowed to move in the specified directions we always have a polyhedral subdivision, but only a power diagram when the back ends of the arrows intersect inside the triangle.

5. THE MORSE POSET

In [SvM04] we introduced the Morse poset for Voronoi diagrams. Here we generalize the Morse poset, so that it is defined for power diagrams.

Consider the function

$$g = \min_{1 \leq i \leq N} g_i(x)$$

This function is a topological Morse function. When does it have a critical point?

THEOREM **7.** *The function g does not have critical points outside the convex hull of* $\{P_1, \cdots, P_N\}$.

Proof. Let x be a point outside the convex hull of $\{P_1, \cdots, P_N\}$. Hyperplanes in $T_x\mathbb{R}^n$ can be identified with affine hyperplanes in $\mathbb{R}^n$ that pass through x. Choose a hyperplane H in x that is parallel to some hyperplane that separates x from $\mathrm{CH}(\{P_1, \cdots, P_N\})$. It follows that all gradients $\frac{\partial g_i}{\partial x} = x - P_i$ point outward from x at one side of H. Thus the function $\min_i g_i$ does not have a critical point at x. $\qquad\square$

Consider the coherent triangulation dual to a power diagram. In the special case of a Delaunay triangulation we have defined a poset of active simplices in the triangulation. They were defined using the critical points of $\min g_i$. We repeat the procedure for power diagrams.

First define the separator of a cell $\alpha \in \mathrm{Del}(\{P_1, \cdots, P_N\})$. The separator $\mathrm{Sep}(\alpha)$ of α is the intersection of all the separators of P_i and P_j such that $\{P_i, P_j\} \subset \alpha$. If α is a vertex then the separator is defined to be just the whole of $\mathbb{R}^n$. Also, for a polyhedron P in $\mathbb{R}^{n+1}$ the relative interior is the interior of the polyhedron as a subset of the affine span $\mathrm{Aff}(P)$ of P. If $\dim \alpha > 0$ then put

(4) $$c(\alpha) = \mathrm{Sep}(\alpha) \cap \mathrm{Aff}(\alpha)$$

For a vertex put $c(\{i\}) = P_i$. We call the simplex in the coherent triangulation *active* if

- $c(\alpha)$ is contained in the relative interior $\mathrm{Interior}(\mathrm{CH}(\alpha))$ of $\mathrm{CH}(\alpha)$, and
- $g(c(\alpha)) = g_i(c(\alpha))$ for some $P_i \in \alpha$

With this definition it might well happen that a vertex is not active. Here is a typical counter intuitive example. Take three points, say $P_1 = (-1, 0)$, $P_2 = (1, 1)$ and $P_3 =$

$(1, -1)$. Then place a large circle around P_1: $r_1 = 5$. Place two smaller circles around P_2 and P_3: $r_2 = \sqrt{\frac{3}{4}}$ and $r_3 = \sqrt{\frac{5}{6}}$. If we look from below at the graph of $\min g_i$ we see a picture alike the one in figure 5. The *Morse poset* of $\{(P_i, w_i)\}_{i=1,\cdots,N}$ consists of the
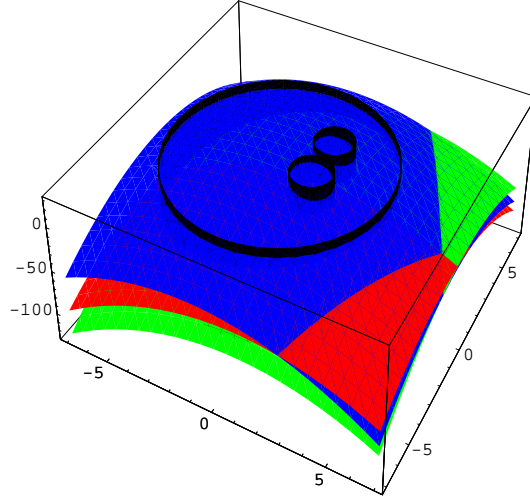

FIGURE 5. Typical counterintuitive example

active subsets of the coherent triangulation. We write

$$g_\alpha(x) = \min_{i \in \alpha} g_i(x) \text{ and } f_\alpha(x) = \max_{i \in \alpha} f_i(x)$$

THEOREM **8.** *There is a one to one correspondence between critical points of $\min_i g_i$ and active cells in the coherent triangulation. An active cell of dimension d corresponds to a critical point of index d.*

Proof. The function $g(x) = \min_i g_i(x)$ can only have a critical point at x_0 when at least two of the $g_i(x_0)$ are equal to $g(x)$. The index set for which $g_i(x_0) = g(x_0)$ is the face α. The function can also only have a critical point when $x_0 \in \text{CH}(\alpha)$. We can thus assume $x_0 = c(\alpha)$.

The index of the critical point can be calculated with theorem 2.3 in [APS97]. First note that for all $x \in \mathbb{R}^n$ the Hessian of $g_i(x)$ is always the unit matrix $\mathbf{I}$.

Consider the subspace

$$T(x) = \cap_{i \in \alpha} \ker \frac{\partial g_i}{\partial x}(x_0) = \cap_{i \in \alpha} \ker(x - P_i)$$

Clearly $T(c(\alpha))$ has the same dimension as $\text{Sep}(\alpha)$. The dimension of T is $n - \dim \alpha$.

The index of the critical point is n minus the dimension of $T(x)$, it is thus the dimension of α.

Conversely if α is active then g_α restricted to $\text{CH}(\alpha)$ has a supremum at $c(\alpha)$.

$$g(x) \le g_\alpha(x) \le g_\alpha(c(\alpha)) \quad \forall x \in \text{CH}(\alpha)$$

Also there is a neighborhood U of $c(\alpha)$ where $g(x) = g_\alpha(c(\alpha))$ and so g has a critical point of index $\dim(\alpha)$.

Note that the reasoning is independent of genericity conditions. $\square$

Finally we remark that though power diagrams are affinely defined, activity is not retained under affine volume preserving linear transformations. Through such transformations the power diagram and its dual coherent triangulation do not change. The Morse poset though, can change drastically after an affine transformation.

6. Discrete Morse theory

We recall the main definitions of the discrete Morse theory developed by Forman. A very good introduction to the subject is [For02]. We show that, though the coherent triangulation is not in general a simplicial complex, it has another nice property: for every two faces $\alpha \subset \gamma$ with $2 + \dim(\alpha) = \dim(\gamma)$ all there are two faces β of the coherent triangulation in between α and γ. Hence, discrete Morse functions on the coherent triangulation have the same nice properties as discrete Morse functions on a simplicial complex.

Let $\mathcal{T}$ be a polyhedral subdivision. By orientating all the faces $\mathcal{T}$ becomes a complex.

DEFINITION **7.** *A function $h: \mathcal{T} \to \mathbb{R}$ is called a* discrete Morse function *if for all $\beta \in \mathcal{T}$*

$$(5) \qquad \#\{\alpha \in \mathcal{T} \mid 1 + \dim(\alpha) = \dim(\beta)\ \alpha \subset \beta\ h(\alpha) \geq h(\beta)\} \leq 1$$

and

$$(6) \qquad \#\{\alpha \in \mathcal{T} \mid \dim(\alpha) = 1 + \dim(\beta)\ \beta \subset \alpha\ h(\alpha) \leq h(\beta)\} \leq 1$$
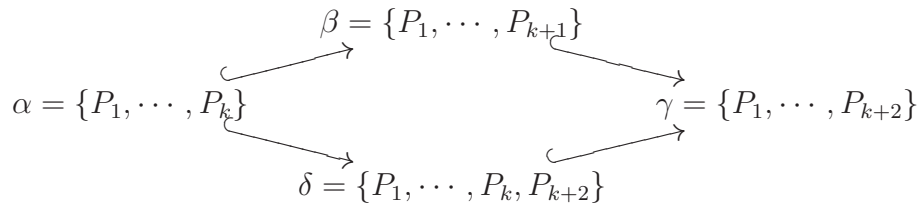
In case both numbers are zero for some $\beta \in \mathcal{T}$, β is called critical.

Analogous to the case of a power diagram and its dual coherent triangulation, we can define a Morse poset of a discrete Morse function h as the set of critical faces of h.

If the power diagram is in general position $\mathcal{T}$ is a simplicial complex. Discrete Morse function on a simplicial complex have a very nice property, see lemma 2.6 in [For98]. If α is a face of β and β is a face of γ. Label the vertices:

$$\alpha = \{P_1, \cdots, P_k\} \quad \beta = \{P_1, \cdots, P_{k+1}\} \quad \gamma = \{P_1, \cdots, P_{k+2}\}$$

Because we are dealing with a simplicial complex there is another face between α and γ: $\delta = \{P_1, \cdots, P_k, P_{k+2}\}$:

$$\beta = \{P_1, \cdots, P_{k+1}\}$$
$$\alpha = \{P_1, \cdots, P_k\} \qquad \qquad \gamma = \{P_1, \cdots, P_{k+2}\}$$
$$\delta = \{P_1, \cdots, P_k, P_{k+2}\}$$

Let f be a discrete Morse function on the simplicial complex. Suppose that $f(\alpha) \geq f(\beta) \geq f(\gamma)$, that is both (5) and (6) hold. We also have $f(\alpha) < f(\delta) < f(\gamma)$, or

$$f(\gamma) > f(\delta) > f(\alpha) \geq f(\beta) \geq f(\gamma)$$

This is a contradiction, so we see that on simplicial complexes at most one (5) and (6) can hold.

However this argument is not restricted to simplicial complexes. All that is needed is that if α and γ are two cells with $\alpha \subset \gamma$ and $2 + \dim \alpha = \dim \gamma$ then there are at least two cells in between α and γ.

THEOREM **9.** *For a coherent triangulation σ as in the above between any two cells α and γ with $2 + \dim \alpha = \dim \gamma$ and $\alpha \subset \gamma$ there are β_1 and β_2, both cells in the coherent triangulation, both having dimension $1 + \dim \alpha$ such that $\alpha \subset \beta_i \subset \gamma$.*

Proof. Consider the cone $\mathrm{Cone}(\gamma, \alpha)$ of γ over α:

$$\mathrm{Cone}(\gamma, \alpha) \overset{\text{def}}{=} \{\beta \mid \alpha \subseteq \beta \subseteq \gamma\}$$

Intersect that cone with the $n - k + 1$ dimensional plane through zero and orthogonal to the $k - 1$-dimensional plane affinely spanned by α. The intersection is a cone in the two dimensional plane. It has two extremal vectors ξ_1 and ξ_2. These correspond to the faces β_1 and β_2 we were looking for. $\qquad\square$

Hence even if the coherent triangulation we have is not a triangulation then we still have that not both (5) and (6) can hold.

If we mod out $\mathrm{Cone}(\gamma, \alpha)$ by the directions $\mathrm{Aff}(\alpha)$ along α we get a vertex of a polyhedron and the faces between α and γ are the edges of a connected fan. So if we have that there can be any number of β_{i1} and β_{i2} between α and γ.

$$\alpha \rightarrow \left\{ \begin{matrix} \beta_{11} \subset \beta_{11} \\ \vdots \quad \vdots \quad \vdots \\ \beta_{l1} \subset \beta_{l1} \end{matrix} \right\} \rightarrow \gamma$$

On any coherent triangulation there exists a discrete Morse function: $h \colon \alpha \mapsto \dim \alpha$. So let us have a discrete Morse function h on the coherent triangulation. The gradient of h consists of arrows $\alpha \rightarrow \beta$, drawn when $\alpha \subset \beta$ and $h(\alpha) \geq h(\beta)$. In general such a collection of arrows is called a *discrete vectorfield*. A V-path is a sequence of arrows such that the simplex pointed to contains a second simplex that points to another one, of higher dimension. A *closed V-path* is a circular V-path as in equation (7). Theorem 3.5 in [For02] states that a discrete vectorfield is the gradient of a discrete Morse function if and only if it contains no closed V-paths.

$$(7) \qquad\qquad \alpha_1 \rightarrow \beta_1 \supset \alpha_2 \rightarrow \beta_2 \supset \cdots \supset \alpha_k \rightarrow \beta_k \supset \alpha_1$$

The dual to the coherent triangulation, the power diagram, is also a polyhedral complex. Given a discrete Morse function $\mathfrak{g}$ on the coherent triangulation, clearly $-\mathfrak{g}$ is a discrete Morse function on the power diagram.
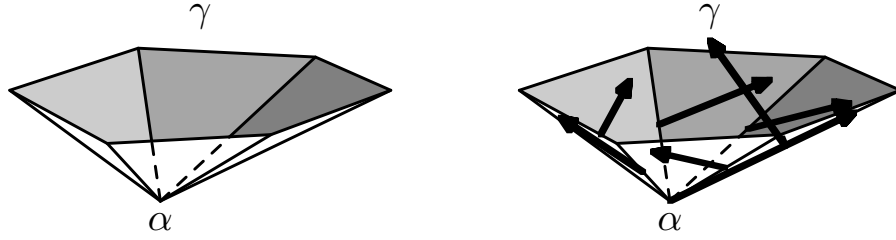
FIGURE 6. A cone of simplices filled up with a discrete vectorfield

7. FROM MORSE POSET TO A DISCRETE VECTORFIELD

In this section we will prove the main new theorem of this article.

THEOREM 10. *On* $\mathrm{Del}(\{P_1, \cdots, P_N\})$ *there exists a discrete Morse function h such that the Morse poset of h equals the Morse poset of $g(x) = \min_{1 \leq i \leq N} g_i(x)$.*

In fact we will not construct h directly. Instead we will construct a discrete vectorfield without closed V-paths. In the reasoning below we disregard the disappearing faces.

A face α can be non-active for one of two reasons

<u>Down</u> The separator $\mathrm{Sep}(\alpha)$ can lie outside $\mathrm{Interior}(\mathrm{CH}(\alpha))$, or if that is not the case:

   <u>Up</u> Some point $P_i \in \{P_1, \cdots, P_N\} \setminus \alpha$ can lie closer to $c(\alpha)$ then the points in α, i.e.

$$(8) \qquad g_i(c(\alpha)) \leq g_j(c(\alpha)) \quad \forall j \in \alpha$$

Suppose that α is not active for the "Down" reason. Then in the case of Voronoi diagrams α cannot be a vertex or an edge. In general with power diagrams α cannot be a vertex.

Suppose that α is not active for the "Up" reason and that $\dim \mathrm{Del}(\alpha) = n$. Then we have

$$\{c(\alpha)\} = \cap_{j \in \alpha} \mathrm{Pow}(\{P_j\}):$$

we cannot have (8). We conclude that no α, not active for the "Up"-reason has $\dim \mathrm{Del}(\alpha) = n$.

We start by showing that for every face, not active for the "Down" reason, there is a unique lower dimensional simplex not active for the "Up" reason. Then we construct for each face not active for the "Up" reason a part of the discrete vectorfield.

LEMMA 2. *Let $\beta \in \mathrm{Del}(\{P_1, \cdots, P_N\})$ be a face not active for the "Down"-reason. Then the closest point to $\mathrm{CH}(\beta)$ from $c(\beta)$ is $c(\alpha)$ for some proper face α of β. At $c(\alpha)$ we have*

$$(9) \qquad g_j(c(\alpha)) \leq g_\alpha(c(\alpha)) \quad \forall j \in \beta \setminus \alpha$$

Hence α is not active for the "Up"-reason. Conversely if (9) holds for $\beta \supset \alpha$ then β is not active for the "Down"-reason.

Proof. We start with "⇒".

A special case we first have to handle is when $c(\beta)$ lies on the relative boundary of $\mathrm{CH}(\beta)$. This means that $c(\beta) \in \mathrm{CH}(\alpha)$ for some proper face α of β. Because $\mathrm{Sep}(\beta) \subset \mathrm{Sep}(\alpha)$ it follows that $c(\beta) = c(\alpha)$. Equation (9) follows automatically.

Now we can safely assume that the distance from $c(\beta)$ to $\mathrm{CH}(\beta)$ is > 0. Denote y the closest point on $\mathrm{CH}(\beta)$ from $c(\beta)$. If α is a vertex we are done, so suppose that α is not a vertex. The line from y to $c(\beta)$ is orthogonal to $\mathrm{Aff}(\alpha)$ and hence parallel to $\mathrm{Sep}(\alpha)$. Clearly $c(\beta)$ lies in $\mathrm{Sep}(\alpha)$. So y also lies in $\mathrm{Sep}(\alpha)$. But y also lies in $\mathrm{Aff}(\alpha)$. So, by the definition of $c(\alpha)$ in equation (4) we have that $y = c(\alpha)$.

Because $\mathrm{CH}(\beta)$ is a convex set the hyperplane with normal $c(\beta) - c(\alpha)$ passing through $c(\alpha)$ separates $\mathrm{Interior}(CH(\beta))$ from $c(\beta)$. Thus the angle P_k to $c(\alpha)$ to $c(\beta)$ must be obtuse. Consequently:

$$(10) \qquad\qquad \|c(\beta) - P_k\| \geq \|c(\beta) - c(\alpha)\| + \|c(\alpha) - P_k\|$$

if P_k is a vertex in $\beta \supset \alpha$. By Pythagoras, equality holds if $k \in \alpha$:

$$(11) \qquad\qquad \|c(\beta) - P_k\| = \|c(\beta) - c(\alpha)\| + \|c(\alpha) - P_k\|$$

Then equation (10) becomes, taking the factor $\frac{1}{2}$ we used in the definition of g in equation (1) into account:

$$(12) \qquad\qquad g_k(c(\beta)) \geq \frac{1}{2}\|c(\beta) - c(\alpha)\| + g_k(c(\alpha)) \quad k \in \beta \setminus \alpha$$

Again, equality holds when $k \in \alpha$. Putting this together we get (9), and we see that α is not active for the "Up"-reason.

Next do the "$\Leftarrow$" part. We assume (9) and $\alpha \subset \beta$. From (9) we get for $j \in \beta \setminus \alpha$:

$$(13) \qquad g_j(c(\alpha)) + \frac{1}{2}\|c(\beta) - c(\alpha)\| \leq g_\alpha(c(\alpha)) + \frac{1}{2}\|c(\beta) - c(\alpha)\| = g_\alpha(c(\beta)) = g_j(c(\beta))$$

The special case to handle first is where equality holds in (13). Then $c(\beta) = c(\alpha)$ and so $c(\beta)$ is not an element of the relative interior $\mathrm{Interior}(\mathrm{CH}(\beta))$. So β is not active for the "Down"-reason.

Now we can safely assume strict inequality in (13). The simplest case is a β for which $\beta = \alpha \cup \{j\}$. The three points P_j, $c(\beta)$ and $c(\alpha)$ all lie in $\mathrm{Aff}(\beta)$. From (13) we get (10) with strict inequality. The line segment from $c(\alpha)$ to $c(\beta)$ is thus an outward normal to $\mathrm{CH}(\beta)$ in $\mathrm{Aff}(\beta)$. Consequently β is not active for the "Down"-reason. The general case is similar. $\qquad\qquad\square$

Let again α be not active for the "Up"-reason. Denote K the set of indices for which (8) holds. Denote $\mathrm{Up}(\alpha)$ the set of simplices:

$$(14) \qquad\qquad \mathrm{Up}(\alpha) = \{\beta \in \mathrm{Del}(\{P_1, \cdots, P_N\}) \mid \alpha \subset \beta \subset \alpha \cup K\}$$

Lemma 2 characterizes the elements of $\mathrm{Up}(\alpha)$ as those $\beta \supset \alpha$ for which $c(\alpha)$ is the closest point on $\mathrm{CH}(\beta)$ from $c(\beta)$. The complement of the Morse poset is divided into different subsets $\mathrm{Up}(\alpha)$, one for each face not active for the "Up"-reason.

In $\mathrm{Up}(\alpha)$ identify those faces δ such that there are no γ in $\mathrm{Up}(\alpha)$ with δ a proper face of γ. Then we see that $\mathrm{Up}(\alpha)$ contains different cones $\mathrm{Cone}(\delta, \alpha)$. These cones can be filled up by a discrete vectorfields, as is shown in figure 6. It is possible to take a number of simplicial cones such that no discrete vectorfield exists that fills up these cones completely. For instance, take two triangles: $\{P_1, P_2\}$, $\{P_1, P_2, P_3\}$ and $\{P_1, P_2, P_4\}$. Obviously there

is no way to fill these cones up with a discrete vectorfield. Therefore, we need to prove that $\mathrm{Up}(\alpha)$ can be filled up with a discrete vectorfield.

We will establish another criterion for which a $\beta \in \mathrm{Del}(\{P_1, \cdots, P_N\})$ with $\alpha \subset \beta$ is an element of $\mathrm{Up}(\alpha)$. Take the point $c(\alpha)$ outside the polytope $\mathrm{Pow}(\alpha)$ in $\mathrm{Sep}(\alpha)$ and consider the faces of $\mathrm{Pow}(\alpha)$ for which the outward pointing normal makes an angle smaller than 90 degrees with $x - c(\alpha)$. Then we get a number of faces $\beta_1, \cdots, \beta_l$ in the Delaunay triangulation that we see as faces $\mathrm{Pow}(\beta_1), \cdots, \mathrm{Pow}(\beta_l)$ on the relative boundary $\partial(\mathrm{Pow}(\alpha))$ of $\mathrm{Pow}(\alpha)$. This is illustrated in figure 7. A precise formulation is
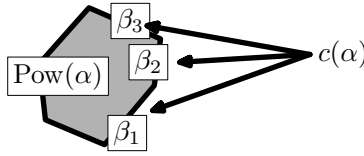

FIGURE 7. View from $c(\alpha)$ to $\mathrm{Pow}(\alpha)$

contained in the following lemma.

LEMMA 3. *Let $\beta \supset \alpha$ be an element of* $\mathrm{Del}(\{P_1, \cdots, P_N\})$. *Let x be a point in the interior of* $\mathrm{Pow}(\beta)$. *If, either $x = c(\alpha)$, or*

(1) *the line through x and $c(\alpha)$ intersects $\mathrm{Pow}(\alpha)$ in a segment, and*
(2) *the segment $[x, c(\alpha)]$ contains no point of the interior of $\mathrm{Pow}(\alpha)$*

then $\beta \in \mathrm{Up}(\alpha)$. Conversely, if 1 and 2 hold for some $\beta \supset \alpha$, with α not active for the "Up"-reason, then $\beta \in \mathrm{Up}(\alpha)$.

Proof. We first need to treat the case $x = c(\alpha)$. In that case $c(\alpha)$ lies on the relative boundary of $\mathrm{Pow}(\alpha)$. So $x \in \mathrm{Pow}(\beta)$, $\beta = \alpha \cup I$. And $f_j(c(\alpha)) = f_\alpha(c(\alpha))$, for all $j \in I$. Obviously $\mathrm{Up}(\alpha)$ consists exactly of all those $\gamma \in \mathrm{Del}(\{P_1, \cdots, P_N\})$ with

$$\alpha \subseteq \gamma \subseteq \beta = \alpha \cup I$$

Now we can assume $x \neq c(\alpha)$. Again x lies on the relative boundary of $\mathrm{Pow}(\beta)$ and $\beta = \alpha \cup I$ for some maximal set I. We put $x_t = tx + (1 - t)c(\alpha)$. Hence $x_1 = x$ and $x_0 = c(\alpha)$. It also follows for $j \in I$

$$f_j(x_t) = tf_j(x) + (1 - t)f_j(c(\alpha)) = tf_\alpha(x) + (1 - t)f_j(c(\alpha))$$

and thus

$$f_j(x_t) - f_\alpha(x_t) = (1 - t)(f_j(c(\alpha)) - f_\alpha(c(\alpha)))$$

Now we have

$$f_j(c(\alpha)) \geq f_\alpha(c(\alpha)) \Leftrightarrow \exists t > 1 : f_j(x_t) \leq f_\alpha(x_t)$$

So that

$$\exists t > 1 \ x_t \in \mathrm{Pow}(\alpha) \Rightarrow f_j(c(\alpha)) \geq f_\alpha(c(\alpha))$$

And this is exactly what we needed to prove.

Now suppose that $\beta \supset \alpha$, and α not active for the "Up"-reason, but that 1 and 2 do not hold.

The only point of $\mathrm{Pow}(\alpha)$ on the line through x and $c(\alpha)$ is x. It follows that $\beta \setminus \alpha$ contains more than one index, i.e. $\beta = \alpha \cup \{j_1, \cdots, j_r\}$ with $r \geq 2$. In a sufficiently small neighborhood of x the halfspaces $H_i = \{f_{j_i} \leq f_\alpha\}$ define $\mathrm{Pow}(\alpha)$ as a polyhedron in $\mathrm{Sep}(\alpha)$. Because $\{x_t \mid t \in \mathbb{R}\}$ touches $\mathrm{Pow}(\alpha)$ there exist an index k, say $k = j_1$, and a $t < 1$ such that $f_j(x_t) - f_\alpha(x_t)$ and hence $f_k(c(\alpha)) < f_\alpha(c(\alpha))$. And so $\beta \supset \alpha$ is not an element of $\mathrm{Up}(\alpha)$. $\qquad\square$

From lemma 3 we see that we can fill up $\mathrm{Up}(\alpha)$ with arrows of a discrete vectorfield. Indeed, with its dual on $\mathrm{Pow}(\alpha)$ we can obviously do this because it is contractible, so we can also do it with $\mathrm{Up}(\alpha)$.

We conclude that the complement of the Morse poset can be divided into separate parts $\mathrm{Up}(\alpha)$, for all α not active for the "Up"-reason. Each of these parts cones represents what Matveev calls a polyhedral collapse in [Mat03]. To show that we indeed get a discrete vectorfield we need to prove one more thing: there should be no closed V-path.

Suppose that we have a closed V-path. Inside one $\mathrm{Up}(\alpha)$ there is no such closed V-path, so at some simplex the V-path should jump from one $\mathrm{Up}(\gamma_1)$ to another $\mathrm{Up}(\gamma_2)$, as in figure 8.
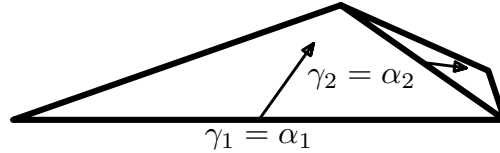

FIGURE 8. A V-path, with a jump from $\mathrm{Up}(\gamma_1)$ to $\mathrm{Up}(\gamma_2)$.

LEMMA **4.** *Suppose that we have a V-path that jumps from $\mathrm{Up}(\gamma_1)$ to $\mathrm{Up}(\gamma_2)$ as in equation* (15).

$$
(15) \qquad
\begin{array}{ccccc}
\alpha_i & \to & \beta_i & \subset & \mathrm{Cone}(\gamma_1 \cup I_1, \gamma_1) \\
 & & \cup & & \\
\alpha_{i+1} & \to & \beta_{i+1} & \subset & \mathrm{Cone}(\gamma_2 \cup I_2, \gamma_2)
\end{array}
$$

Then $g_{\gamma_1}(c(\gamma_1)) > g_{\gamma_2}(c(\gamma_2))$.

Proof. Because γ_1 is a proper subset of $\gamma_1 \cup \gamma_2$ we see that: $c(\gamma_1 \cup \gamma_2) \notin \mathrm{Interior}(\mathrm{CH}(\gamma_1 \cup \gamma_2))$. The closest point to $\mathrm{CH}(\gamma_1 \cup \gamma_2)$ from $c(\gamma_1 \cup \gamma_2)$ is $c(\gamma_1)$, as we have shown in lemma 2. In particular

$$
(16) \qquad \|c(\gamma_1 \cup \gamma_2) - c(\gamma_1)\| < \|c(\gamma_1 \cup \gamma_2) - c(\gamma_2)\|
$$

Here, the inequality is strict. The closest point is unique, because $\mathrm{CH}(\gamma_1 \cup \gamma_2)$ is convex.
For the reasons explained in the proof of lemma 2 we have

$$
(17) \qquad g_{\gamma_1 \cup \gamma_2}(c(\gamma_1 \cup \gamma_2)) = g_{\gamma_1}(c(\gamma_1 \cup \gamma_2)) = \frac{1}{2}\|c(\gamma_1 \cup \gamma_2) - c(\gamma_1)\| + g_{\gamma_1}(c(\gamma_1))
$$

The same identity holds with γ_1 and γ_2 exchanged, thus:

$$(18) \qquad \frac{1}{2}\|c(\gamma_1 \cup \gamma_2) - c(\gamma_1)\| + g_{\gamma_1}(c(\gamma_1)) = \frac{1}{2}\|c(\gamma_1 \cup \gamma_2) - c(\gamma_2)\| + g_{\gamma_2}(c(\gamma_2))$$

Putting (16) and (18) together we get the desired result. $\qquad\square$

Lemma 4 says that to each $\mathrm{Up}(\alpha)$ appearing in the V-path we can associate a number, and passing from one $\mathrm{Up}(\alpha)$ to another that number strictly decreases. Hence we can not have a closed V-path. The proof of theorem 10 is complete.

REMARK **3.** *We are not entirely satisfied with the proof of our main theorem. What is lost in the proof is a direct relation between g and the discrete Morse function that gives the discrete vectorfield we construct. We tried using $\alpha \to \sup_{x \in \mathrm{CH}(\alpha)} g(x)$ as a function on the coherent triangulation but this approach did not give the desired results.*

REMARK **4.** *We were neither entirely satisfied with discrete Morse theory, because it seems to be ill equipped for dealing with polyhedral collapses: our vectorfield is not unique. The non-uniqueness only lies in the choice of the arrows possible in $\mathrm{Up}(\alpha)$. One could also try to develop a generalization of discrete Morse theory in order to include polyhedral collapses.*

8. EXAMPLES

Let us return to the counterintuitive example of figure 5. There the Morse poset is as in figure 9. In the picture we see three cones, consisting each of two faces in the simplest triangulation one can think of.
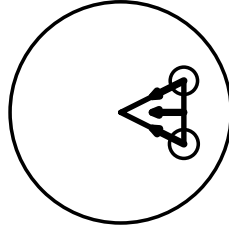

FIGURE 9. Morse poset and discrete vectorfield of figure 5

Another example is the one called $4300I$ in our previous article [SvM04]. Let the active subsets be $\{\{P_1, P_2\}, \{P_2, P_3\}, \{P_3, P_4\}\}$. Then if $\alpha = \{P_1, P_2, P_3, P_4\}$ the face $\{P_1, P_4\}$ is not active for the "Up"-reason. In that case both $\{P_1, P_3, P_4\}$ and $\{P_1, P_2, P_4\}$ and $\{P_1, P_2, P_3, P_4\}$ are not active for the "Down" reason. There is one cone consisting of the polyhedral collapse:

$$\{P_1, P_4\} \to \{P_1, P_2, P_4\} \quad \{P_1, P_3, P_4\} \to \{P_1, P_2, P_3, P_4\}$$

The decomposition of that cone into arrows is not unique. We might just as well write

$$\{P_1, P_4\} \to \{P_1, P_3, P_4\} \quad \{P_1, P_2, P_4\} \to \{P_1, P_2, P_3, P_4\}$$

Another application is the classification of all Morse posets of Voronoi diagrams for 4 points in the plane in [Sie99]. Unfortunately there were two cases missing, which are now included in figure 10.
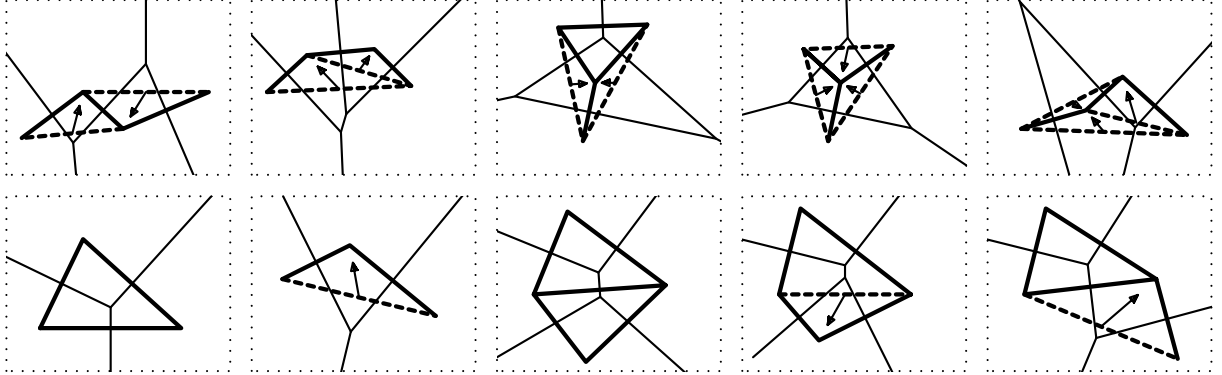

FIGURE 10. 3 and 4 points in $\mathbb{R}^2$: all Morse posets from Voronoi diagrams with the accompanying discrete vectorfields

9. THE MEDIAL AXIS AND MASLOV DEQUANTIZATION

It is well known that the medial axis of a compact embedded submanifold M in $\mathbb{R}^n$ can be calculated as an approximation of a Voronoi diagram, see for instance [ABK98]. We use tropical geometry to give a new interpretation of that fact. Recall that the *corner locus* of a convex function f is the set of points where f is not differentiable.

We have seen in the above that the Voronoi diagram can also be calculated using the affine functions f_i, instead of the distance function. The corner locus of the function

$$f(x) = \max_i \langle x, P_i \rangle - \frac{1}{2}\|P_i\|$$

is the Voronoi diagram. It is natural to try the same procedure with the embedding $\gamma \colon M \to \mathbb{R}^n$. We will show next that the medial axis is a corner locus as well.

PROPOSITION 4. *Let M be a compact smooth manifold, embedded by $\gamma \colon M \to \mathbb{R}^n$ in $\mathbb{R}^n$. Write for $s \in M$:*

$$f_s(x) = \langle x, \gamma(s) \rangle - \frac{1}{2}\|\gamma(s)\|$$

The function f defined by

$$(19) \qquad f(x) \stackrel{\text{def}}{=} \sup_{s \in M} f_s(x) = \lim_{h \to \infty} \frac{\log\left(\int_M h^{f_s(x)} ds\right)}{\log(h)}$$

is a convex function, and satisfies the stated equality. Its corner locus is the medial axis of M.

Proof. The function $f(x)$ is convex, because it is the supremum of a number of convex functions. Because M is compact the supremum is attained for one or more points $s = s(x)$ in M. We see that $x \in \mathbb{R}^n$ and $s \in M$, for which $f(x) = f_s(x)$, are related by

$$(20) \qquad \langle x - \gamma(s), \dot{\gamma}(s) \rangle = 0$$

I.e. x lies on the normal of one or more $s \in M$. Of those that satisfy (20) we choose one that has the highest value of $f_{s_i}(x)$, and thus the lowest value of

$$\frac{1}{2}\|x\| - f_{s_i}(x) = \frac{1}{2}\|x - \gamma(s_i)\|$$

The s we get from $\sup_{s \in M} f_s$ corresponds to the point closest to x on the submanifold M. And the points where $f(x)$ is not differentiable form exactly the medial axis of M. It remains to prove the formula for $\sup_{s \in M} f_s$ in (19).

For this we use the so-called Maslov dequantization. Maslov dequantization is a fancy name for the identity:

$$(21) \qquad \lim_{h \to \infty} \log_h(h^a + h^b) = \max(a, b)$$

that holds for any two real numbers a and b. $\qquad \square$

For practical purposes this procedure works well. The integrals can in most cases not be calculated explicitly, but if one uses numerical integration one can plot f, as is illustrated in figure 11.
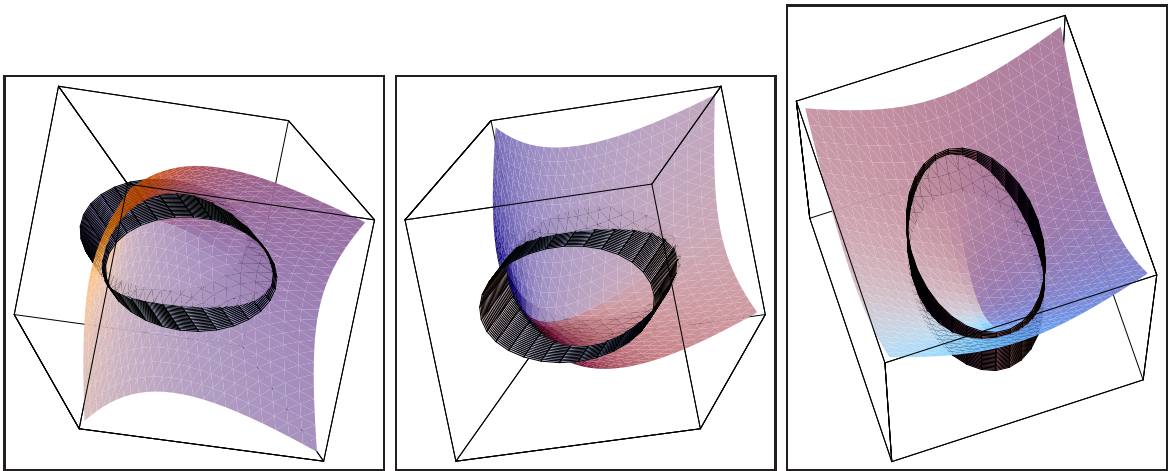

FIGURE 11. The graph of $\sup_{s \in M} f_s(x)$ when γ is the ellipse.

The Maslov dequantization as in equation (21) is strongly related to a construction in toric geometry, described in [Ful93], section 4.2. Namely, let again

$$f_i(x) = \langle x, P_i \rangle + c_i \qquad i = 1, \cdots, N$$

be affine functions defining a power diagram. Define the following function

$$H \colon \mathbb{R}^n \to \mathbb{R}^n \quad H(x) = \frac{\sum_{i=1}^N P_i e^{f_i(x)}}{\sum_{i=1}^N e^{f_i(x)}}$$

It is proved in [Ful93] that H is a real analytic diffeomorphism from $\mathbb{R}^n$ to the interior of $CH(\{P_1, \cdots, P_N\})$, when that interior is not empty. One recognizes H as a gradient:

$$H(x) = \frac{\partial}{\partial x} \left(\log \left(\sum_{i=1}^N e^{f_i(x)} \right) \right)$$

Now consider the gradient:

$$H_h(x) = \frac{\partial}{\partial x} \left(\log_h \left(\sum_{i=1}^N h^{f_i(x)} \right) \right) = \frac{\sum_{i=1}^N P_i h^{f_i(x)}}{\sum_{i=1}^N h^{f_i(x)}}$$

PROPOSITION **5.** *Suppose that the interior of* $CH(\{P_1, \cdots, P_N\})$ *is not empty. The map* H_h *is a real analytic diffeomorphism from* $\mathbb{R}^n$ *to the interior of* $CH(\{P_1, \cdots, P_N\})$.

Proof. The f_i are of the form $\langle x, P_i \rangle + c_i$. Put $\tilde{f}_i(u) = \langle u, P_i \rangle + \log(h) c_i$. We already know that

$$u \longrightarrow \tilde{H}(u) = \frac{\sum_{i=1}^N P_i e^{\tilde{f}_i(u)}}{\sum_{i=1}^N e^{\tilde{f}_i(u)}}$$

is a real analytic diffeomorphism from $\mathbb{R}^n$ to the interior of $CH(\{P_1, \cdots, P_N\})$. Because we have $H_h(x) = \tilde{H}(x \log(h))$ the proof is complete. $\qquad \square$

Taking infinitely many points and a Riemann sum we see that the gradient of the function $\log_h \left(\int_M h^{f_s(x)} ds \right)$ is a diffeomorphism from $\mathbb{R}^n$ to the region in $\mathbb{R}^n$ bounded by the compact embedded manifold $M \subset \mathbb{R}^n$. Now in the limit $h \to \infty$, the image of M is the medial axis. This is another way of saying that the dual of the medial axis in the sense of the theorem of Passare and Rullgård is the manifold M itself.

REFERENCES

[ABK98]   Nina Amenta, Marshall Bern, and Manolis Kamvysselis, *A new voronoi-based surface reconstruction algorithm*, SIGGRAPH '98: Proceedings of the 25th annual conference on Computer graphics and interactive techniques (New York, NY, USA), ACM Press, 1998, pp. 415–421.

[AI87]   Franz Aurenhammer and Hiroshi Imai, *Geometric relations among Voronoĭ diagrams*, STACS 87 (Passau, 1987), Lecture Notes in Comput. Sci., vol. 247, Springer, Berlin, 1987, pp. 53–65. MR MR900443

[APS97]   A. A. Agrachev, D. Pallaschke, and S. Scholtes, *On Morse theory for piecewise smooth functions*, J. Dynam. Control Systems **3** (1997), no. 4, 449–469. MR **MR1481622 (98m:**49034)

[Aur87]   F. Aurenhammer, *Power diagrams: properties, algorithms and applications*, SIAM J. Comput. **16** (1987), no. 1, 78–96. MR **MR873251 (88d:**68096)

[DFG02]   D.-E. Diaconescu, B. Florea, and A. Grassi, *Geometric transitions, del Pezzo surfaces and open string instantons*, Adv. Theor. Math. Phys. **6** (2002), no. 4, 643–702. MR **MR1969655 (2005a:**81206)

[For98]   Robin Forman, *Morse theory for cell complexes*, Adv. Math. **134** (1998), no. 1, 90–145. MR **MR1612391 (99b:**57050)

[For02]   ———, *A user's guide to discrete Morse theory*, Sém. Lothar. Combin. **48** (2002), Art. B48c, 35 pp. (electronic). MR **MR1939695 (2003j:**57040)

[Ful93]   William Fulton, *Introduction to toric varieties*, Annals of Mathematics Studies, vol. 131, Princeton University Press, Princeton, NJ, 1993, The William H. Roever Lectures in Geometry. MR **MR1234037 (94g:**14028)

[GKZ94]   I. M. Gel′fand, M. M. Kapranov, and A. V. Zelevinsky, *Discriminants, resultants, and multidimensional determinants*, Mathematics: Theory & Applications, Birkhäuser Boston Inc., Boston, MA, 1994. MR **MR1264417 (95e:**14045)

[Hör94]   Lars Hörmander, *Notions of convexity*, Progress in Mathematics, vol. 127, Birkhäuser Boston Inc., Boston, MA, 1994. MR **MR1301332 (95k:**00002)

[Lin02]   Roderik Cornelis Lindenbergh, *Limits of Voronoi diagrams*, Rijksuniversiteit te Utrecht, Utrecht, 2002, Dissertation, Universiteit Utrecht, Utrecht, 2002. MR **MR1925090 (2003g:**52027)

[Man39]   Szolem Mandelbrojt, *Sur les fonctions convexes*, C. R. Acad. Sci. Paris **209** (1939), 977–978. MR MR0000846 (1,137b)

[Mat03]   Sergei Matveev, *Algorithmic topology and classification of 3-manifolds*, Algorithms and Computation in Mathematics, vol. 9, Springer-Verlag, Berlin, 2003. MR **MR1997069 (2004i:**57026)

[Pen03]   Hélène Pennaneac′h, *Tropical geometry and amoebas*, Unpublished manuscript (2003), 22.

[PR04]   Mikael Passare and Hans Rullgård, *Amoebas, Monge-Ampère measures, and triangulations of the Newton polytope*, Duke Math. J. **121** (2004), no. 3, 481–507. MR **MR2040284 (2005a:**32005)

[RGST03]   Jürgen Richter-Gebert, Bernd Sturmfels, and Thorsten Theobald, *First steps in tropical geometry*, arXiV.math **AG.0306366** (2003), 1–29.

[Sie99]   D. Siersma, *Voronoi diagrams and Morse theory of the distance function*, Geometry in Present Day Science, World Scientific, Singapore, 1999, pp. 187–208.

[SvM04]   Dirk Siersma and Martijn van Manen, *The nine morse generic tetrahedra*, arXiV.math **MG.0410251** (2004), 1–14.

[Zie95]   Günter M. Ziegler, *Lectures on polytopes*, Graduate Texts in Mathematics, vol. 152, Springer-Verlag, New York, 1995. MR **MR1311028 (96a:**52011)

MATHEMATISCH INSTITUUT, UNIVERSITEIT UTRECHT, PO Box 80010, 3508 TA UTRECHT THE NETHERLANDS.
   E-mail address: `siersma@math.uu.nl`

DEPARTMENT OF MATHEMATICS, HOKKAIDO UNIVERSITY KITA 10, NISHI 8, KITA-KU, SAPPORO, HOKKAIDO, 060-0810, JAPAN
   E-mail address: `manen@math.sci.hokudai.ac.jp`